

# **Sensitivity Analysis for a Pyrotechnically Actuated Pin Puller Model\***

Joseph M. Powers<sup>†</sup> and Keith A. Gonthier<sup>‡</sup>

Department of Aerospace and Mechanical Engineering  
University of Notre Dame  
Notre Dame, Indiana 46556-5637  
USA

## **Abstract**

This paper gives an analysis which determines the parametric sensitivity of a recently developed pyrotechnic model. The model is used to predict the dynamic events associated with the combustion of a pyrotechnic charge in the NASA Standard Initiator (NSI) actuated pin puller. The model is formulated as a set of ordinary differential equations and solved to determine system performance. Using an experimentally verified pressure-time prediction as a baseline, the sensitivity of the kinetic energy imparted to the pin as a function of system parameters is studied. The results illustrate the usefulness of the model for predicting the performance of pyrotechnic devices and also suggest that beyond certain limits a precise knowledge of model parameters is not necessary in order to evaluate the pin puller performance.

## **Introduction**

Recently, Gonthier and Powers (1993) developed a model to predict the behavior of a pyrotechnically actuated pin puller. Through the use of uncertain, yet plausible, modeling assumptions and parameter estimations, they were able to achieve reasonable agreement with experimental observations. In order to quantify the sensitivity of the results to variations in some of the uncertain parameters, this study was performed. For completeness, we first summarize the motivation and model development as originally given by Gonthier and Powers. This includes a description of the device and mathematical model, baseline model predictions and comparisons with experiments for the pin puller. We then give the new results of the sensitivity study.

---

\* This paper is submitted, July 1993, for presentation at the Nineteenth International Pyrotechnics Seminar, Christchurch, New Zealand, February 1994. The study is supported by the NASA Lewis Research Center under Contract Number NAG-1335. Dr. Robert M. Stubbs is the contract monitor.

<sup>†</sup> Assistant Professor, corresponding author.

<sup>‡</sup> Graduate Research Assistant.

## Basic Operation of Pin Puller

Figure 1 depicts a cross-section of a standard pyrotechnically actuated pin puller in its unretracted state (Bement, *et al.*, 1991). The primary pin is driven by gas generated by combustion of a pyrotechnic within a device known as the NASA Standard Initiator (NSI). The pyrotechnic consists of a mixture of approximately 114 mg of zirconium fuel (53.6 mg Zr) and potassium perchlorate oxidizer (60.4 mg  $KClO_4$ ). Initially a thin diaphragm encloses the pyrotechnic. Combustion of the pyrotechnic is initiated by the transfer of heat from an electric bridgewire to the pyrotechnic. Upon ignition, the pyrotechnic undergoes rapid chemical reaction producing both condensed phase and gas phase products. The high pressure products accelerate the gas generation rate, burst the confining diaphragm, then vent through the port into the expansion chamber. Once in the chamber, the high pressure gas first causes shear pins to fail, then pushes the primary pin. After the pin is stopped by crushing an energy-absorbing cup, the operation of the device is complete. Peak pressures within the expansion chamber are typically around 7,000 psi [48.25 MPa]. Completion of the stroke requires about 0.5 ms.

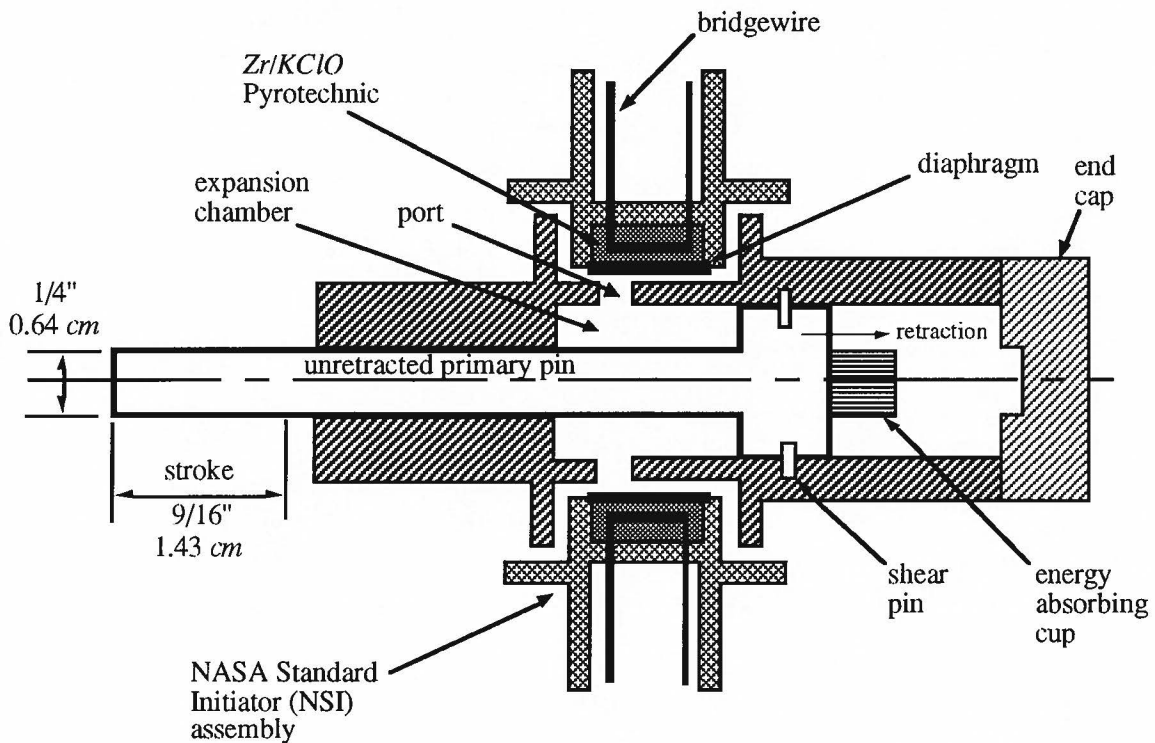


Figure (1). Cross-sectional view of pyrotechnically actuated pin puller.

## Model Description

Assumptions adopted for the model are as follows. As depicted in Figures (2a,b), the total system is taken to consist of three subsystems: incompressible solid pyrotechnic reactants (*s*), incompressible condensed phase products (*cp*), and gas phase products (*g*). Mass and heat exchange between subsystems is allowed such that 1) mass can be

transferred from the solid pyrotechnic to both the condensed phase and gas phase products, and 2) heat can be transferred between the condensed phase and gas phase products. The gas phase subsystem is also allowed to interact across the system boundary with its surroundings in the form of heat and work exchanges. In this case the surroundings are taken to consist of an isothermal cylindrical container bounded at one end by a movable, frictionless piston. There is no mass exchange between the surroundings and any of the subsystems. No work exchange between subsystems is allowed, nor is any heat transfer modeled between the solid pyrotechnic and either product subsystem. Spatial variations within subsystems are neglected; consequently, all variables are only time-dependent and the total system is modeled as a well-stirred reactor. The kinetic energy of the subsystems is ignored, while an accounting is made of the kinetic energy of the bounding piston. Body forces are neglected.

The rate of exchange of mass from the reactant subsystem to the gas and condensed phase product subsystems is taken to be related to the gas phase pressure. In the absence of reliable data for  $Zr-KClO_4$ , reaction rates have been estimated to be in the same range as those of typical solid rocket propellants as given by Barrere, *et al.*, (1960). Predictions from the equilibrium thermochemistry algorithm CET89 (Gordon and McBride, 1976) calculated for constant volume complete combustion of the  $Zr-KClO_4$  mixture are used to estimate the instantaneous product composition. It is assumed that the instantaneous mass fractions of the many gas phase products and one condensed phase product are known constants given by the CET89 calculation. Thus, the reaction products satisfy the condition that in a constant volume combustion process the Gibbs free energy is minimized. The component gases are taken to be ideal with temperature-dependent specific heats. The specific heats are in the form of fourth-order polynomial curve fits given by the CET89 code and not repeated here.

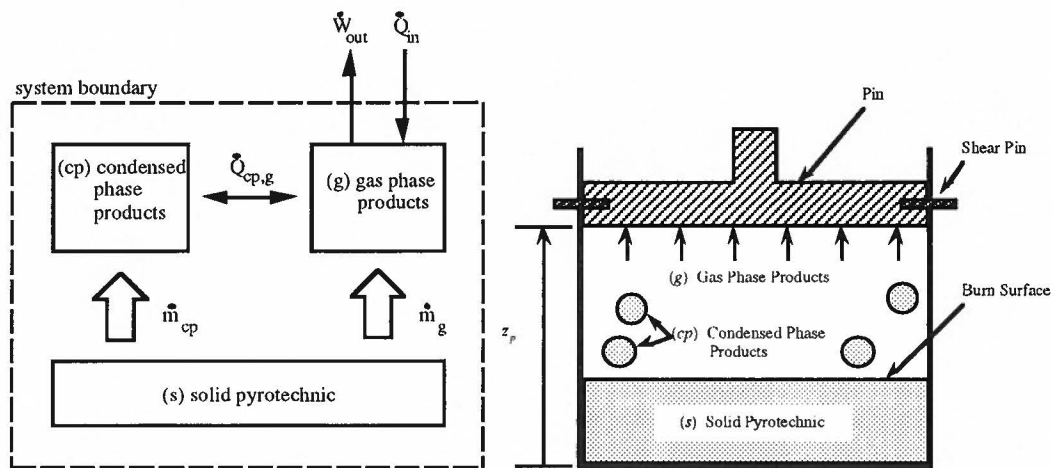


Figure (2a,b). Mass and heat transfer interactions between various subsystems.

With these assumptions a model can be written using principles of two-phase reactive flow such as those described by Powers, *et al.*, (1990a,b), for related systems. Other models for pyrotechnic systems have been given by Farren, *et al.* (1986). Razani, *et al.* (1990), and Butler, *et al.* (1993). Evolution of mass and energy for each subsystem along

with an equation of motion for the pin are written below as a set of non-dimensional ordinary differential equations:

$$\frac{d}{dt}[\rho_s V_s] = -\rho_s r, \quad (1)$$

$$\frac{d}{dt}[\rho_{cp} V_{cp}] = \eta_{cp} \rho_s r, \quad (2)$$

$$\frac{d}{dt}[\rho_g V_g] = (1 - \eta_{cp}) \rho_s r, \quad (3)$$

$$\frac{d}{dt}[\rho_s V_s e_s] = -\rho_s e_s r, \quad (4)$$

$$\frac{d}{dt}[\rho_{cp} V_{cp} e_{cp}] = \eta_{cp} \rho_s e_s r - \dot{Q}_{cp,g}, \quad (5)$$

$$\frac{d}{dt}[\rho_g V_g e_g] = (1 - \eta_{cp}) \rho_s e_s r + \dot{Q}_{in} + \dot{Q}_{cp,g} - \dot{W}_{out}, \quad (6)$$

$$\frac{d^2}{dt^2}[z_p] = \left[ \frac{\tilde{F}_c}{\tilde{m}_p \tilde{V}_c^{1/3} / \tilde{t}_c^2} \right] F_p. \quad (7)$$

The independent variable in Eqs. (1-7) is time  $t$ . The dependent variables are the product gas density  $\rho_g$ , the internal energies per unit mass  $e_s$ ,  $e_{cp}$ ,  $e_g$ , the volumes  $V_s$ ,  $V_{cp}$ ,  $V_g$ , the pin position  $z_p$ , the linear pyrotechnic burn rate  $r$ , the rate of heat transfer from the condensed phase products to the gas phase products  $\dot{Q}_{cp,g}$ , the rate of heat transfer from the surroundings to the system  $\dot{Q}_{in}$ , the rate of work done by the products in moving the pin  $\dot{W}_{out}$ , and the net force acting on the pin  $F_p$ . Constant parameters are the pin mass  $\tilde{m}_p$ , the unreacted solid pyrotechnic density  $\rho_s$ , the condensed phase product density  $\rho_{cp}$ , and the mass fraction of the products which are in the condensed phase  $\eta_{cp}$ .

Equations (1-3) describe the evolution of mass of the solid pyrotechnic, condensed phase products, and gas phase products, respectively. Eqs. (1-3) are constructed such that when added, the total systems' mass is conserved. Equations (4-6) describe the evolution of energy for the solid pyrotechnic, condensed phase products, and gas phase products, respectively. They are constructed such that when added, the total systems' energy changes only due to heat and work exchanges with the surroundings. Equation (7) is the equation of motion for the pin.

Equations (1-7) have been scaled such that all thermodynamic variables and time are  $O(1)$  quantities at the completion of the combustion process. Dimensional quantities are indicated by the notation “ $\sim$ ”. Characteristic dimensional scales, denoted by subscript “ $c$ ”, are given by:

$$\begin{aligned}
\tilde{V}_c &= \tilde{V}_{so}, & \tilde{\rho}_c &= (1 - \eta_{cp}) \left( \frac{\tilde{V}_{so}}{\tilde{V}_o} \right) \tilde{\rho}_s, & \tilde{T}_c &= \tilde{T}_{ad}, & \tilde{e}_c &= \tilde{e}_{so}, \\
\tilde{P}_c &= (1 - \eta_{cp}) \left( \frac{\tilde{V}_{so}}{\tilde{V}_o} \right) \tilde{\rho}_s \tilde{R} \tilde{T}_{ad}, & \tilde{F}_c &= \tilde{A}_p (1 - \eta_{cp}) \left( \frac{\tilde{V}_{so}}{\tilde{V}_o} \right) \tilde{\rho}_s \tilde{R} \tilde{T}_{ad}, \\
\tilde{r}_c &= \tilde{b} \left[ (1 - \eta_{cp}) \left( \frac{\tilde{V}_{so}}{\tilde{V}_o} \right) \tilde{\rho}_s \tilde{R} \tilde{T}_{ad} \right]^n, & \tilde{t}_c &= \frac{\tilde{V}_{so}}{\tilde{A}_p \tilde{b} \left[ (1 - \eta_{cp}) \left( \frac{\tilde{V}_{so}}{\tilde{V}_o} \right) \tilde{\rho}_s \tilde{R} \tilde{T}_{ad} \right]^n}.
\end{aligned} \tag{8}$$

Additional parameters appearing in Eqs. (8) are the initial solid pyrotechnic volume  $\tilde{V}_{so}$ , the initial total system volume  $\tilde{V}_o$ , the adiabatic flame temperature for the reaction  $\tilde{T}_{ad}$ , the mass-averaged equivalent gas constant for the gas phase products  $\tilde{R}$ , the pin cross-sectional area, which is also the area of the burning surface,  $\tilde{A}_p$ , and characteristic burn rate constants  $\tilde{b}$  and  $n$ .

Geometrical and constitutive relations necessary to close Eqs. (1-7) are given by the following:

$$V = V_s + V_{cp} + V_g, \tag{9}$$

$$z_p = \left( \frac{\tilde{V}_{so}^{2/3}}{\tilde{A}_p} \right) V, \tag{10}$$

$$P_g = \rho_g T_g, \tag{11}$$

$$r = r(P_g) = P_g^n, \tag{12}$$

$$e_s(T_s) = \sum_{i=1}^{N_s} Y_{s_i} e_{s_i}(T_s), \tag{13}$$

$$e_{cp}(T_{cp}) = \sum_{i=1}^{N_{cp}} Y_{cp_i} e_{cp_i}(T_{cp}), \tag{14}$$

$$e_g(T_g) = \sum_{i=1}^{N_g} Y_{g_i} e_{g_i}(T_g), \tag{15}$$

$$c_{v_s}(T_s) = \sum_{i=1}^{N_s} Y_{s_i} \frac{d}{dT_s} [e_{s_i}(T_s)], \tag{16}$$

$$c_{v_{cp}}(T_{cp}) = \sum_{i=1}^{N_{cp}} Y_{cp_i} \frac{d}{dT_{cp}} [e_{cp_i}(T_{cp})], \quad (17)$$

$$c_{v_g}(T_g) = \sum_{i=1}^{N_g} Y_{g_i} \frac{d}{dT_g} [e_{g_i}(T_g)], \quad (18)$$

$$\dot{Q}_{cp,g} = \dot{Q}_{cp}(T_{cp}, T_g) = \left[ \frac{\tilde{h}_{cp,g} \tilde{T}_c}{\tilde{\rho}_c \tilde{A}_p \tilde{r}_c \tilde{e}_c} \right] (T_{cp} - T_g), \quad (19)$$

$$\dot{Q}_{in} = \dot{Q}_{in}(T_g) = \left[ \frac{\tilde{h} \tilde{V}_c^{2/3} \tilde{T}_c}{\tilde{\rho}_c \tilde{A}_p \tilde{r}_c \tilde{e}_c} \right] A_w (T_w - T_g) + \left[ \frac{\tilde{\sigma} \tilde{V}_c^{2/3} \tilde{T}_c^4}{\tilde{\rho}_c \tilde{A}_p \tilde{r}_c \tilde{e}_c} \right] A_w (\alpha T_w^4 - \varepsilon T_g^4), \quad (20)$$

$$A_w = \left[ 2 \sqrt{\frac{\pi \tilde{V}_c^{2/3}}{\tilde{A}_p}} \right] (V - V_s), \quad (21)$$

$$\dot{W}_{out} = \left[ \frac{\tilde{P}_c}{\tilde{\rho}_c \tilde{e}_c} \right] P_g \frac{dV}{dt}, \quad (22)$$

$$F_p = \begin{cases} 0 & \text{if } P_g < F_{crit} \\ P_g & \text{if } P_g \geq F_{crit} \end{cases}. \quad (23)$$

Equations (9) and (10) are geometrical constraints. Here,  $V$  is the total volume. Equation (11) is a thermal equation of state for the gas phase combustion products. The pressure-dependent pyrotechnic combustion rate  $r$  is given by Eq. (12). In this expression,  $n$  is an empirically determined constant. This rate is similar in form to those used for solid propellant combustion modeling.

Caloric equations of state for the solid pyrotechnic, condensed phase products, and gas phase products are given by Eqs. (13), (14), and (15), respectively. Here,  $T_s$  is the temperature of the solid pyrotechnic, and  $T_{cp}$  is the temperature of the condensed phase products. Also  $Y_{s_i}$ ,  $Y_{cp_i}$ ,  $Y_{g_i}$ ,  $N_s$ ,  $N_{cp}$ , and  $N_g$  are the mass fractions and number of component species of solid pyrotechnic, condensed phase product, and gas phase products, respectively. The subscript  $i$  is used to denote an individual species. From earlier-stated assumptions, each is assumed to be a known constant from the CET89 calculation. Since for both ideal gases and condensed phase species, the internal energy is only a function of temperature, the specific heat at constant volume for the solid pyrotechnic  $c_{vs}$ , the condensed phase products  $c_{vcp}$ , and the gas phase products  $c_{vg}$  can be obtained via term-by-term differentiation of the above caloric equations of state with respect to temperature. Expressions for the specific heats at constant volume are given by Eqs. (16), (17), and (18).

Equation (19) gives an expression for the rate of heat transfer from the condensed phase products to the gas phase products. In this expression,  $\tilde{h}_{cp,g}$  is a constant heat

transfer parameter. The heat transfer rate from the gas phase products to the surroundings, given by Eq. (20), assumes two modes of heat transfer: convective and radiative. Constant parameters in this equation are the convective heat transfer coefficient  $\tilde{h}$ , the absorptivity of the vessel's walls  $\alpha$ , the emissivity of the gas  $\varepsilon$ , the Stefan-Boltzmann constant  $\tilde{\sigma}$ , and the vessel's wall temperature  $T_w$ . Here  $A_w$  is the instantaneous surface area of the vessel's walls. Equation (21) relates  $A_w$  to  $V$  and  $V_s$  for a cylindrical vessel.

Equation (22) models pressure-volume work done by the expanding gas in moving the pin. Equation (23) models the force acting on the pin due to the gas phase pressure and a restraining force due to the shear pins which are used to initially hold the pin in place. Here  $F_{crit}$  is the critical force necessary to cause shear pin failure. The work associated with shearing the pin is not considered.

In summary, Eqs. (1-23) represent a coupled system of differential and algebraic equations. Gonthier and Powers give details of how this system can be reduced to a system of six ordinary differential equations in six unknowns of the form:

$$\frac{d\mathbf{u}}{dt} = \mathbf{f}(\mathbf{u}) \quad (24)$$

where  $\mathbf{f}$  is a vector function of the vector of dependent variables  $\mathbf{u}$ , and  $\mathbf{u}$  is the column vector  $[V, V_s, V_{cp}, T_{cp}, T_g, \dot{V}]^T$ . Here  $\dot{V}$  is the first time derivative of the total volume. Six initial conditions for each of these equations are specified as

$$\begin{aligned} V(t=0) &= V_o, & V_s(t=0) &= V_{so}, & V_{cp}(t=0) &= V_{cpo}, \\ T_{cp}(t=0) &= T_o, & T_g(t=0) &= T_o, & \dot{V}(t=0) &= 0. \end{aligned} \quad (25)$$

Here "o" denotes an initial state. Gonthier and Powers go on to show how all other variables can be written as algebraic functions of  $\mathbf{u}$ .

## Results

Numerical solutions were obtained for the simulated firing of an NSI into the pin puller device. The numerical scheme used was an explicit stiff ordinary differential equation solver given in the standard code LSODE. The combustion process predicted by the CET89 chemical equilibrium code obeyed the balanced stoichiometric equation given in Table 1. The parameters chosen and initial conditions are presented in Table 2 and 3, respectively.

### Pin Puller Simulation

Predictions and measurements (Bement, 1992) of pressure-time histories for the pin puller are given in Fig. (3). In the experiments, one port contained the NSI and the other a pressure transducer. Here, we predict a rapid pressure rise up to a maximum value near  $57.9 \text{ MPa}$  occurring about  $0.07 \text{ ms}$  after combustion initiation. Following this maximum, there is a decrease in pressure to a value of  $24.13 \text{ MPa}$  at completion of the stroke ( $0.47 \text{ ms}$ ). The rapid pressure rise is attributable to gases generated during combustion. The

peak pressure occurs near the time of combustion extinction, and the subsequent pressure decay is due to the combined effect of heat transfer to the surroundings and work done by the expanding gas in moving the pin.

Figure (4) illustrates the partitioning of energy between the three subsystems, the kinetic energy of the pin (labeled “work”), and the energy lost to the surroundings as heat. As the combustion proceeds, the energy of the solid pyrotechnic decreases while the energies of both the condensed phase and gas phase products increase. Very little energy is used in moving the pin or lost to the surroundings during this time. Following completion of the combustion process, a larger fraction of the energy is used in retracting the pin. However, for the particular choice of heat transfer parameters used in this study, very little energy is ultimately lost to the surroundings due to heat transfer. The predicted kinetic energy of the pin at completion of the stroke is 27 *J*. Experimentally observed values for the pin kinetic energy at completion of the stroke are typically near 22.6 *J*.

### Model Sensitivity

This section gives results showing the sensitivity of the model to variations in the burn rate parameters  $\tilde{b}$  and  $n$  and the heat transfer parameters  $\tilde{h}$ ,  $\alpha$ ,  $\epsilon$ , and  $\tilde{h}_{cp,g}$ . For this study, we use the predicted pin puller solution as the baseline solution (baseline parameters are given in Table 2). The sensitivity of the model is determined by finding the parametric dependency of the pin kinetic energy at the completion of the stroke.

Model sensitivity to changes in the burn rate parameters  $\tilde{b}$  and  $n$  is shown in Figures (5) and (6), respectively. In these figures, the predicted kinetic energy of the pin at completion of the stroke has been scaled by the total energy released by the combustion process (308.7 *J*). For  $\tilde{b} \geq 3.0 \times 10^{-4} \text{ dyne}^{-0.69} \text{ cm/s}$  or  $n \geq 0.52$ , corresponding to fast burning rates, the predicted kinetic energy of the pin at completion of the stroke is a maximum equaling an approximately constant value of 0.107. For lower values of these parameters, corresponding to slower burning rates, the predicted kinetic energy of the pin at completion of the stroke decreases as the rate of heat transfer to the surroundings becomes more significant.

Model sensitivity to changes in the convective heat transfer coefficient  $\tilde{h}$  and the radiative heat transfer parameters  $\alpha$  and  $\epsilon$  is shown in Figures (7) and (8), respectively. Trends observed in Figure (7) show that for values of  $\tilde{h} \leq 3.0 \times 10^7 \text{ g/s}^3/\text{K}$ , the predicted pin kinetic energy is a maximum. For larger values of this parameter, the pin kinetic energy decreases as the rate of heat transfer to the surroundings increases. Figure (8) shows that the model is insensitive to any changes in  $\alpha$  or  $\epsilon$ .

Model sensitivity to changes in the condensed phase-gas phase heat transfer coefficient  $\tilde{h}_{cp,g}$  is shown in Figure (9). Trends in this figure show that the predicted pin kinetic energy is a maximum for values of  $\tilde{h}_{cp,g} \geq 3.0 \times 10^9 \text{ g cm}^2/\text{s}^3/\text{K}$  and decreases for smaller values of  $\tilde{h}_{cp,g}$ . These trends indicate that the transfer of heat from the condensed phase products to the gas phase products is necessary to provide the gas phase products with sufficient energy to retract the pin.



## Conclusions

The sensitivity analysis shows that the following conditions result in optimal pin puller performance: 1) a fast burning rate, 2) a low convective heat transfer rate from the gas phase products to the surroundings, and 3) a high heat transfer rate from the condensed phase products to the gas phase products.

The model presented in this paper has demonstrated success in predicting the events associated with the firing of pyrotechnically actuated devices. The model correctly predicts time scales and pressure magnitudes. Though the model predicts well variables which are of engineering interest many of the constitutive models are *ad hoc*, though plausible. It is seen however that outside of certain critical zones the variable which is of actual engineering interest, namely the pin's kinetic energy, is insensitive to changes in model parameters. Consequently, it may not be necessary to have a great deal of precision in making estimates for these parameters; only certain bounds need be specified.

## References

Barrere, M., Jaumotte, A., De Veubeke, B. F., and Vandekerckhove, J., 1960, *Rocket Propulsion*, Elsevier, New York.

Bement, L. J., 1992, private communication, NASA Langley Research Center, Hampton, Virginia.

Bement, L. J., Multhaup, H. A., and Schimmel, M.L., 1991, "HALOE Gimbal Pyrotechnic Pin Puller Failure Investigation, Redesign, and Qualification," NASA Langley Research Center, Hampton, Virginia.

Butler, P. B. Kang, J., and Krier, H., 1993, "Modeling Pyrotechnic Combustion in an Automotive Airbag Inflator," *Proceedings - Europyro 93, 5<sup>e</sup> Congres International de Pyrotechnie du Groupe de Travaile*, Strasbourg, France, pp. 61-70.

Farren, R. E., Shortridge, R. G., and Webster, H. A., III, 1986, "Use of Chemical Equilibrium Calculations to Simulate the Combustion of Various Pyrotechnic Compositions," *Proceedings of the Eleventh International Pyrotechnics Seminar*, pp. 13-40.

Gonthier, K. A., and Powers, J. M., 1993, "Model Formulation and Predictions for a Pyrotechnically Actuated Pin Puller," *Proceedings - Europyro 93, 5<sup>e</sup> Congres International de Pyrotechnie du Groupe de Travaile*, Strasbourg, France, pp. 237-248.

Gordon, S., and McBride, B. J., 1976, "Computer Program for Calculation of Complex Chemical Equilibrium Compositions, Rocket Performance, Incident and Reflected Shocks, and Chapman-Jouguet Detonations," NASA SP-273, NASA Lewis Research Center, Cleveland, Ohio.

Powers, J. M., Stewart, D. S., and Krier, H., 1990a, "Theory of Two-Phase Detonation - Part I: Modeling," *Combustion and Flame*, **80**, pp. 264-279.

Powers, J. M., Stewart, D. S., and Krier, H., 1990b, "Theory of Two-Phase Detonation - Part II: Structure," *Combustion and Flame*, **80**, pp. 280-303.

Razani, A., Shahinpoor, M., and Hingorani-Norenberg, S. L., 1990, "A Semi-Analytical Model for the Pressure-Time History of Granular Pyrotechnic Materials in a Closed System," *Proceedings of the Fifteenth International Pyrotechnics Seminar*, pp. 799-813.

Table 1. Balanced stoichiometric equations used in pyrotechnic combustion simulations.

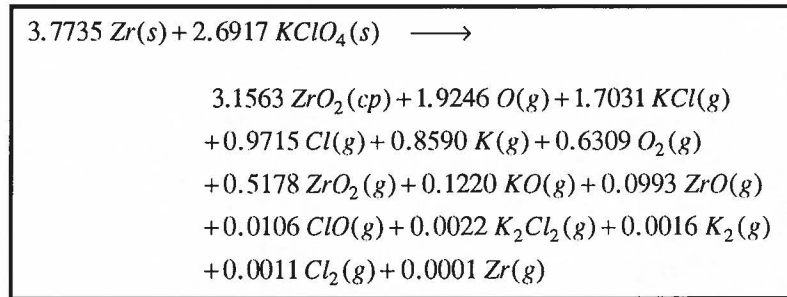


Table 2. Parameters used in pyrotechnic combustion simulations.

parameter	value
$\tilde{A}_p$	$0.64^a \text{ cm}^2$
$\tilde{\rho}_s$	$3.0 \text{ g/cm}^3$
$\tilde{T}_s$	$288.0 \text{ K}$
$\tilde{\rho}_{cp}$	$1.5 \text{ g/cm}^3$
$\tilde{h}$	$1.25 \times 10^6 \text{ g/s}^3/\text{K}$
$\epsilon$	$0.60$
$\alpha$	$0.60$
$\tilde{h}_{cp,g}$	$3.2 \times 10^{10} \text{ g cm}^2/\text{s}^3/\text{K}$
$\tilde{F}_{crit}$	$3.56 \times 10^7 \text{ dyne (80 lbf)}$
$\tilde{b}$	$0.004 \text{ dyne}^{-0.69} \text{ cm/s}$
$n$	$0.69$

Table 3. Initial conditions used in pyrotechnic combustion simulations.

initial condition	value
$V_O$	$21.69$
$V_{SO}$	$1.0$
$V_{cpo}$	$8.56 \times 10^{-5}$
$T_O$	$5.66 \times 10^{-2}$
$\dot{V}_o$	$0.0$

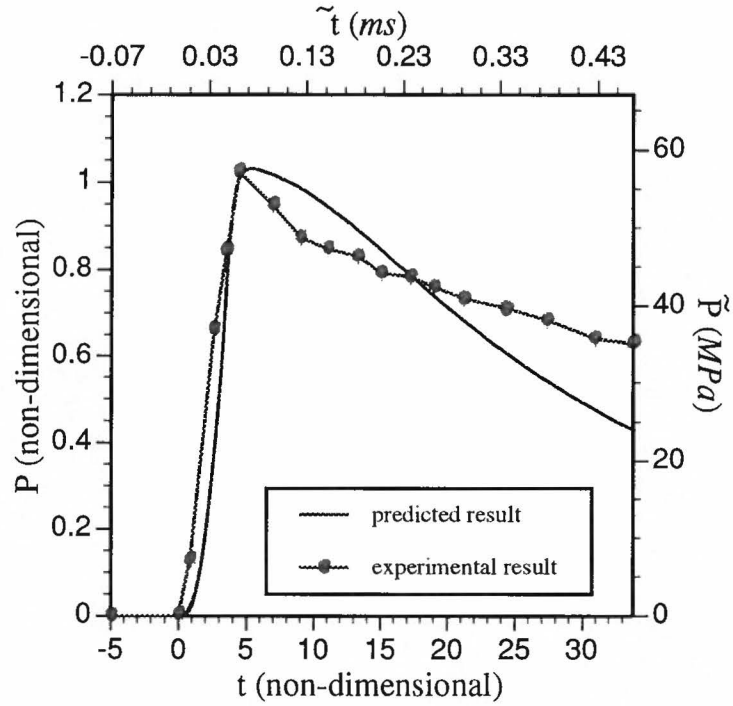


Figure (3). Predicted and experimental pressure histories for the pin puller simulation.

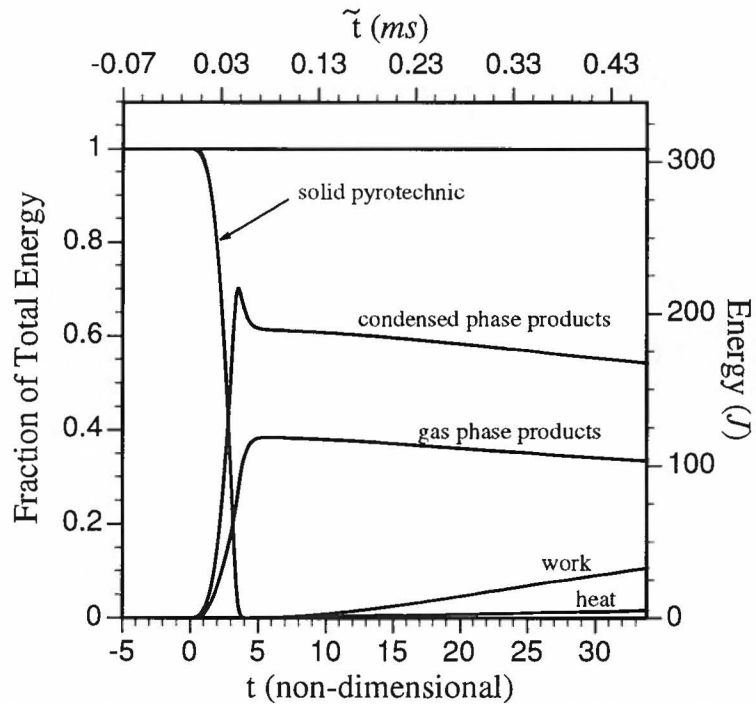


Figure (4). Partitioning of energy for the pin puller simulation.

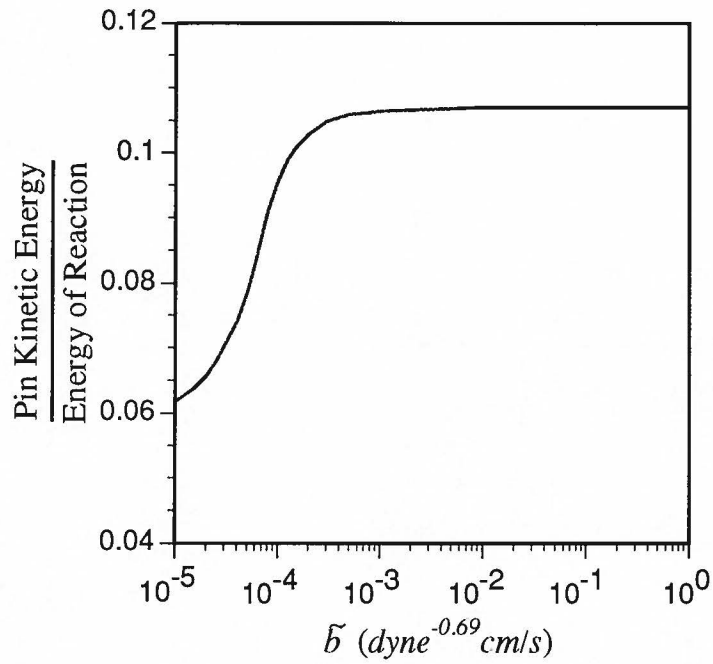


Figure (5). Pin kinetic energy at completion of the stroke for the burn rate parameter study.

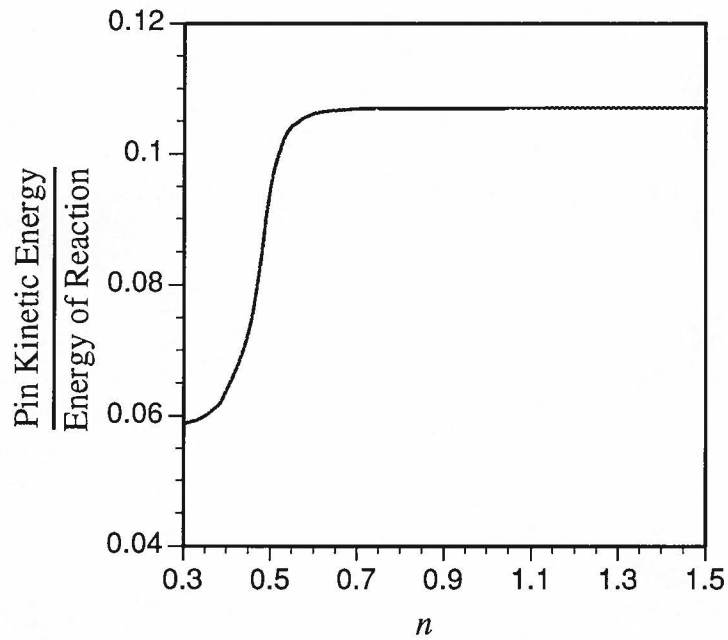


Figure (6). Pin kinetic energy at completion of the stroke for the burn rate parameter study.

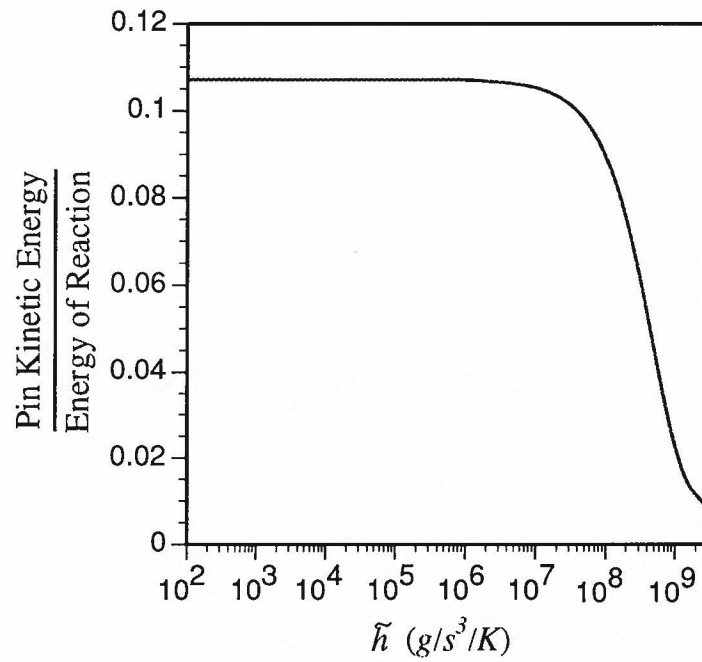


Figure (7). Pin kinetic energy at completion of the stroke for the convective heat transfer coefficient study.

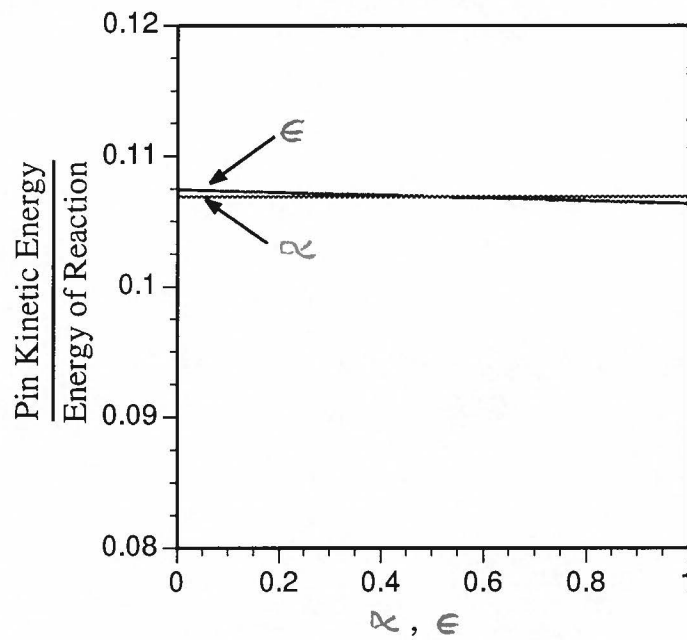


Figure (8). Pin kinetic energy at completion of the stroke for the radiative heat transfer parameter study.

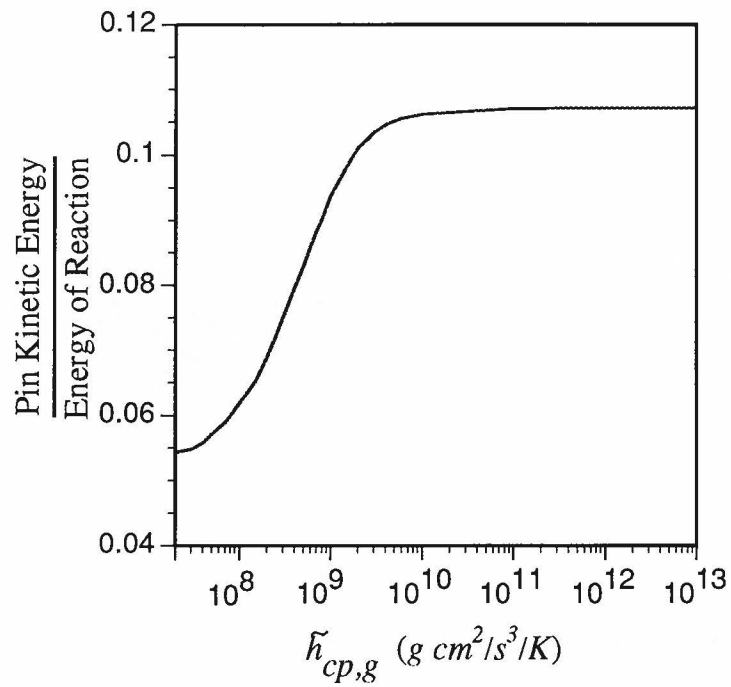


Figure (9). Pin kinetic energy at completion of the stroke for the condensed phase - gas phase product heat transfer coefficient study.